

## DIAGNOSTICS AND ANALYSIS TECHNIQUES FOR HIGH POWER X-BAND ACCELERATING STRUCTURES

A. Degiovanni, S. Doebert, W. Farabolini, I. Syratchev, W. Wuensch, CERN, Geneva, Switzerland  
 J. Giner-Navarro, IFIC and University of Valencia, Spain  
 J. Tagg, National Instruments Switzerland, Ennetbaden, Switzerland  
 B. Woolley, Lancaster University, Lancaster, United Kingdom

### Abstract

The study of high gradient limitations due to RF breakdowns (BD) is extremely important for the CLIC project. A series of diagnostics tools and analysis techniques have been developed in order to monitor and characterize the behaviour of accelerating structures under high power operation in the first CERN X-band klystron-based test stand (Xbox-1). The data collected during the last run on a TD26CC structure [1] are presented in this paper. From the analysis of the RF power and phases, the location of the breakdowns inside the structure could be determined. Other techniques based on the field emitted dark current signals collected by Faraday cups placed at the two extremities of the structure have also been investigated. The results of these analyses are reported and discussed.

### INTRODUCTION

CERN has constructed and is operating a klystron-based X-band test stand, called Xbox-1, dedicated to the high-gradient testing of prototype accelerating structures for CLIC and other applications such as FELs [2]. A TD26CC structure was high-power tested in the Xbox-1 test stand from July to December 2013. The conditioning process was computer controlled using the newly-developed algorithm described in [2].

The accelerating structure was instrumented and interlocked for BD with incident, transmitted and reflected RF signals, Faraday cups and vacuum [1]. A photograph of the experimental setup is shown in fig. 1.

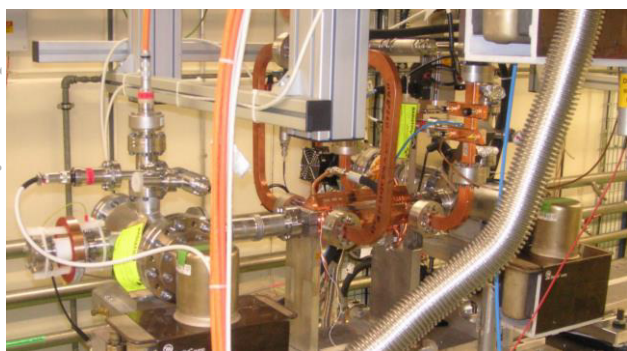


Figure 1: TD26CC structure installed in X-box1.

During breakdowns, a strong field reflection and charge emission can be measured. The data collected during

breakdown events have been analysed in order to determine the breakdown location and to characterize the behaviour of the structure [3, 4]. The difference in timing between the transmitted and reflected signals or the echo between incident and reflected signals method can be used for breakdown cell localization. The emergence of a so-called “hot cell” can then be determined by looking at the distribution of breakdowns along the structure. Such information provides very important feedback for fabrication, conditioning and even the RF design of the structure [5]. For example a concentration of breakdowns could occur due to field profile along the structure.

The results of a breakdown position analysis obtained during the last run of the TD26CC structure are presented in this paper.

### DIAGNOSTICS AND ACQUISITION SYSTEM

RF signals are sampled via 50 dB high power directional couplers and then propagated via N-type coaxial cables to an electronics crate. The signals are then split and sent to log detectors and IQ demodulators. The voltage outputs from the log-detectors are then digitized with 250 MHz Analogue to Digital Converters (ADCs) installed on a National Instruments PXI crate for acquisition and control. The IQ signals are converted to digital signals by 1 GHz ACQIRIS cards and then sent to the PXI crate. Power and phase of the signals are reconstructed from the IQ signals.

The dark current pulses are collected by Faraday cups placed in the downstream (DC1) and upstream (DC2) directions along the structure’s beam axis and then digitized with a 250 MHz ADC. The Faraday cup signals are terminated in 50 Ohms.

The acquisition system stores pulse shapes of breakdown pulses with the previous two normal pulses (for comparison), as well as the pulse shapes of a normal pulse every minute, in order to monitor the behaviour of the accelerating structure. Typical incident, transmitted and reflected power signals, as well as Faraday cup signals during normal operation and for breakdowns are compared in Fig. 2.

As it is visible in Fig. 2, during a breakdown the transmitted power drops, while the reflected power signal increases. The dark current signals increase by a factor 100-1000, saturating the ADCs.

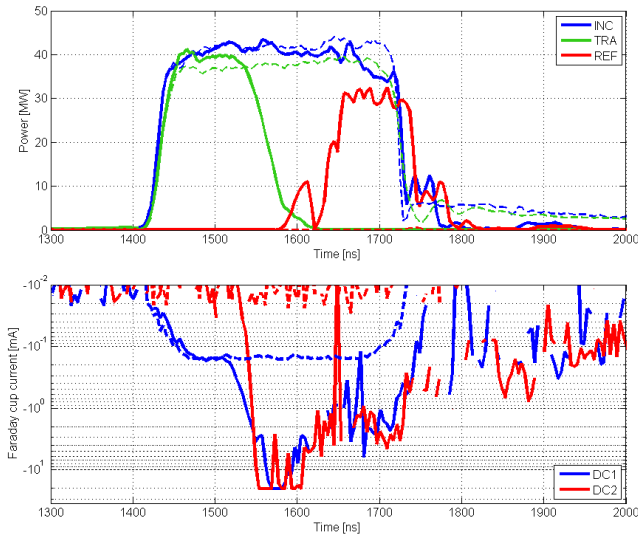


Figure 2: Typical RF signals (top) and dark current signals (bottom) collected during the test of the TD26CC structure in Xbox-1. The dashed lines show the previous pulse signals.

### BREAKDOWN LOCATION

The data collected by the acquisition system were analysed off-line in order to derive the information concerning the position of breakdowns. Three methods were used [3, 6].

The first method consists in looking at the difference in timing between the falling edge of transmitted power ( $t_{T90}$ ) and the rising edge of reflected power ( $t_{R10}$ ). These quantities correspond to the times needed by the RF wave to travel from the breakdown cell ( $n_{BD}$ ) respectively to the downstream and upstream RF couplers. From the group velocity profile  $v_{gr}(n)$  of the structure (Fig. 3) it is possible to translate the time into a measure of the length travelled by the RF wave and finally to the cell location  $n_{BD}$  by using the following equation:

$$t_{R10} - t_{T90} = l_{cell} \left( \sum_0^{n_{BD}} \frac{1}{v_{gr}(n)} - \sum_{n_{BD}}^N \frac{1}{v_{gr}(n)} \right)$$

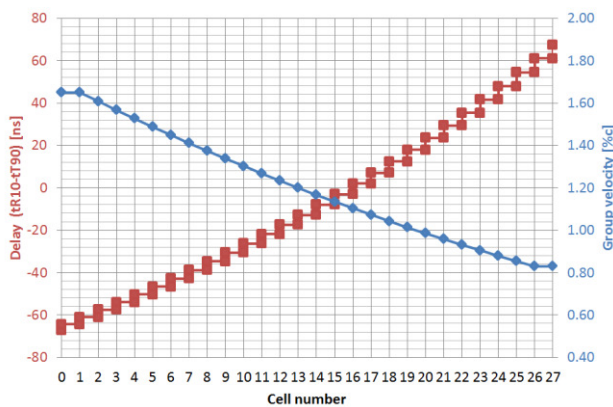


Figure 3: Group velocity profile and equivalent delay times between reflected and transmitted signals.

The second method consists in looking at the correlation between incident and reflected power in the tail of the pulse (when the incident power has dropped to less than 30%). The large currents emitted during the breakdown will usually cause a full reflection of the incident signal. At the end of the RF pulse, the klystron itself will act as a short. The reflected signal will then start to bounce and will be delayed by a time  $t_d$  equal to  $2 \cdot t_{R10}$  and attenuated by a factor  $A$  - which also strongly depends on  $t_d$  (because of the attenuation up and back to the breakdown cell  $n_{BD}$ ). In this case a 2D fit is used to find the pair of signal attenuation and delay that maximizes the correlation between the two signals:

$$t_d(n_{BD}), A(n_{BD}): \max \left[ \text{corr} \left( P_{IN}(t), \frac{P_{REF}(t + t_d)}{A} \right) \right]$$

An example of pulse shapes information used for breakdown location is shown in the top graph of Fig. 4. The black curve on the plot represents what is obtained from the reflected signal after applying the corrections for attenuation and delay. The bottom plot of Fig. 4 shows the phases of the signals, which have been used for the phase distribution study discussed in the next Section.

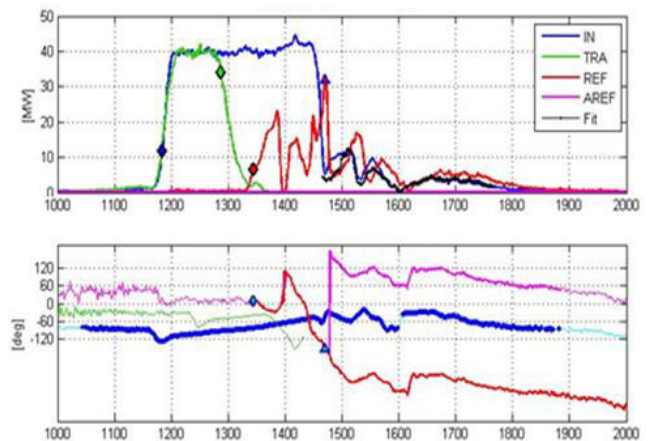


Figure 4: Example of power and phase sampled with IQ demodulators.

The third method of breakdown localization consists in measuring the time difference between the dark current bursts caused by a breakdown and the falling edge of the transmitted power.

The three methods are in good agreement and the results obtained have been used to build a histogram of the BD location during the conditioning process [1].

### PHASE DISTRIBUTION

A subset of 333 BDs collected during the last part of the conditioning phase of the test (at 250 ns pulse width) has been used to analyse the breakdown phase distribution [6].

The phase of the breakdown events (Fig. 4) has been defined as the difference between the phase of the incident signal and the phase of the reflected signal.

Distinct phase jumps occur in more than 40% of the breakdown pulses (Fig. 5). This effect could be caused by either an expansion of the size of the breakdown region or the ignition of secondary breakdowns upstream of the original one.

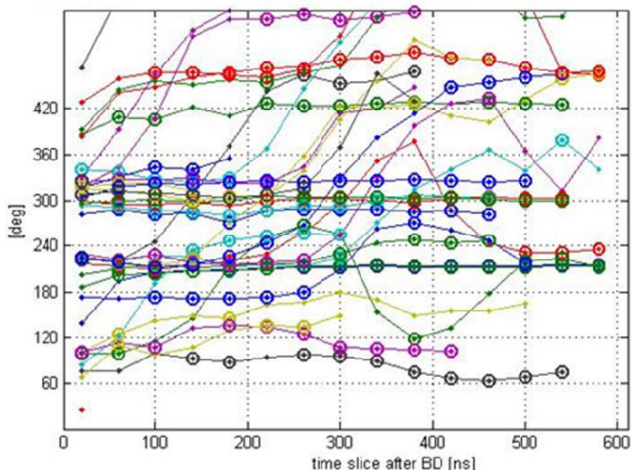


Figure 5: Breakdown phases sampled after the breakdown ignition. About 40% of the traces shows a phase drift which could correspond to a drift of the breakdown or the ignition of a second breakdown.

The measured phases are distributed around three peaks at about  $120^\circ$  of distance (Fig. 6), as it is expected because of the  $2\pi/3$  phase advance between cells [7].

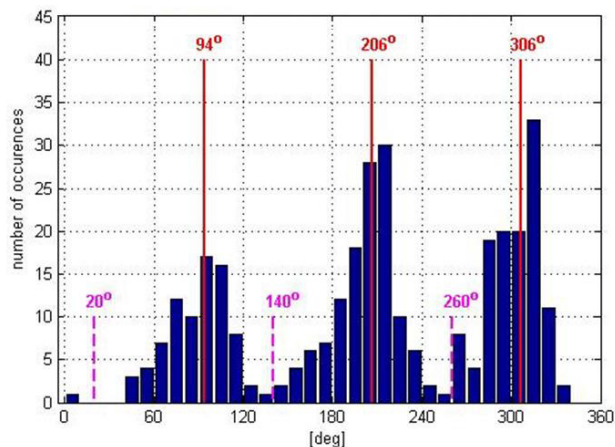


Figure 6: Breakdown phase distribution for a subset of 333 breakdowns measured during the 250 ns run.

The phase information is combined with the time information [6] giving the results shown in Fig. 7. In the plot, the delay and phase pairs corresponding to each iris are indicated by the red dots. The ticks on the right axis show the cell time delays when not using the phase information to refine the location. The horizontal dashed lines are the bins delays used to attribute a breakdown to a given cell when knowing the phase. Looking at the plot of Fig. 7, it is clear that, even with the sampling rate of 1 ns of the IQ signals, the delay method alone is quite sensitive to measurement errors. The use of the phase information makes the bins (the horizontal dashed lines) 3 times

larger, so less sensitive to measurement errors. There is no evidence of a hot cell. On the other hand a detuning slope is visible.

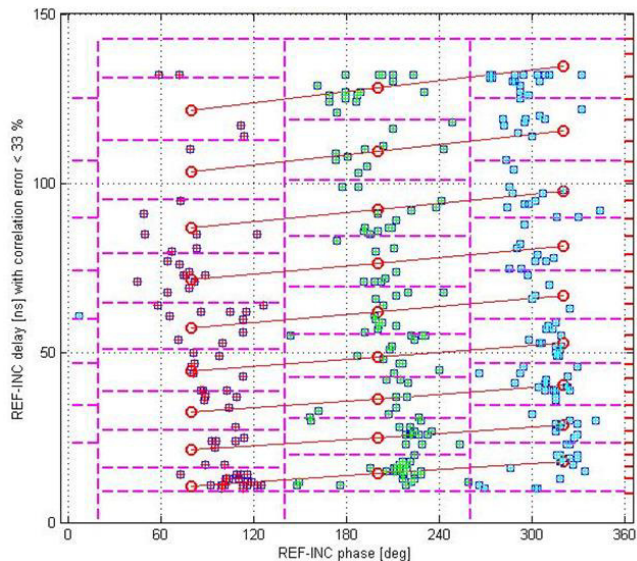


Figure 7: RF signals delay vs. phase for 333 breakdowns.

## CONCLUSION

Diagnostics tools and analysis techniques for the localization of RF breakdowns have been used to study the behaviour of a recently tested CLIC accelerating structure. The algorithms developed for this analysis are based on timing comparisons. Additional information was obtained from the measurement of the RF phase of the reflected signal. The algorithms that have been validated off-line will now be implemented on the control system of the Xbox-1 test stand to monitor on-line the conditioning process of future structures.

## REFERENCES

- [1] A. Degiovanni et al., “High-Gradient Test Results From a CLIC Prototype Accelerating Structure: TD26CC”, IPAC’14, Dresden, June 2014.
- [2] N. Catalan-Lasheras et al., “Experiences Operating an X-Band High-Power Test Stand at CERN” IPAC’14, Dresden, June 2014.
- [3] T. Higo et al., “High Gradient Study at KEK on X-band Accelerator Structure for Linear Collider”, PAC’05, Knoxville, May 2005.
- [4] C. Adolphsen et al., “Processing Studies of X-band Accelerator Structures at the NLCTA”, PAC’01, Chicago, June 2001.
- [5] T. Higo, “Progress of X-band Accelerating Structures”, LINAC’10, Tsukuba, September 2010.
- [6] C. Adolphsen, “Normal-Conducting RF Structure Test Facilities and Results”, SLAC-PUB-9906, 2003.
- [7] A. Palaia et al., Diagnostics of RF Breakdowns in High-Gradient Accelerating Structures, DIPAC’11, Hamburg, May 2011.